Polymer 51 (2010) 5385–5391

Contents lists available at ScienceDirect

Polymer

journal homepage: www.elsevier.com/locate/polymer

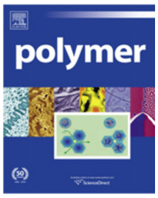

Conjugated copolymers based on dihexyl-benzimidazole moiety for organic photovoltaics

Suhee Song [a], Sung Heum Park [b], Youngeup Jin [c], Il Kim [d], Kwanghee Lee [b], Hongsuk Suh [a,*]

[a] *Department of Chemistry and Chemistry Institute for Functional Materials, Pusan National University, Busan 609-735, Republic of Korea*
[b] *Department of Materials Science and Engineering, Gwangju Institute of Science and Technology, Gwangju 500-712, Republic of Korea*
[c] *Department of Industrial Chemistry, Pukyong National University, Busan 608-739, Republic of Korea*
[d] *The WCU Center for Synthetic Polymer Bioconjugate Hybrid Materials, Department of polymer Science and Engineering, Pusan National University, Busan 609-735, Republic of Korea*

ARTICLE INFO

Article history:
Received 20 July 2010
Received in revised form
10 September 2010
Accepted 14 September 2010
Available online 21 September 2010

Keywords:
Photovoltaic cells
Solubility
2*H*-benzimidazole

ABSTRACT

In this study, we report the synthesis, characterization, and photovoltaic properties of a series of four conjugated polymers based on donor-acceptor (D-A) structure. New polymers, **P1**, **P2**, **P3** and **P4** utilizing a new accepter, dihexyl-2*H*-benzimidazole, were synthesized using Stille coupling reaction. Even with two bithiophene units in the copolymers to facilitate absorption at the longer wavelength, the incorporation of dihexyl-substituent on 2*H*-benzimidazole enables the polymers to have good solubility. The spectra of the solid films show absorption bands with maximum peaks at about 442–479 nm and the absorption onsets at 529–575 nm, corresponding to band gaps of 2.16–2.34 eV. The device with **P4**:$PC_{71}BM$ blend demonstrated an open-circuit voltage (V_{OC}) of 0.59 V, a short-circuit current (J_{SC}) of 6.43 mA/cm^2, and a fill factor (*FF*) of 0.39, leading to the efficiency of 1.46%.

1. Introduction

Organic photovoltaics (OPVs) have been attracting substantial interest due to their significant advantages of low cost, lightweight and favorable solution processability, as well as their potential application in ink-jet printing[1] and roll-to-roll process[2] for flexible large-area devices [3,4]. Since the discovery of the photovoltaic effect in bulk heterojunction (BHJ) devices, there has been an extensive research in polymer solar cells [5]. To achieve high efficiencies, the active layer of polymer solar cells should have a broad and strong absorption in the range of solar spectrum [4]. Various kinds of new low-bandgap polymers have been reported for the enhanced harvest of the solar spectrum, especially in the 1.4–1.9 eV region [6,7].

Many conjugated polymers with electron-rich unit (donor) and electron-deficient unit (acceptor) along their backbone have been widely developed since their absorption spectra and band gap can be readily adjusted by controlling the intramolecular charge transfer (ICT) from the donors to the acceptors. Several donor-acceptor type (D-A) conjugated polymers with narrow band gaps, including poly[*N*-9'-heptadecanyl-2,7-carbazole-*alt*-5,5-(4′,7′-di-2-thienyl-2′,1',3′-benzothiadiazole)] (**PCDTBT**) [7], have shown promising performances with the PCE values as high as 3–6% [6,8].

Hence, to improve harvesting of sunlight, several types of low band gap conjugated polymers were designed, synthesized, and used in polymer solar cells [5,9]. Many of the low-bandgap conjugated polymers with excellent efficiencies have electron-deficient heterocycles, such as benzothiadiazole [10], and electron-rich moieties [11]. Recently, to obtain longer conjugation lengths and backbone coplanarity of the polymers, various kinds of electron-deficient aromatic heterocycles have been widely investigated in OPVs [11]. 2,1,3-Benzothiadiazole and its derivatives, particularly 4,7-di-2-thienyl-2,1,3-benzothiadiazole (DTBT), are the electron-deficient comonomers for the intramolecular charge transfer, which results in the lower band gap of the polymers.

Here, we report new conjugated polymers, **P1**, **P2, P3** and **P4** containing electron donor-acceptor pairs for OPV device utilizing a new type of acceptor, dihexyl-2*H*-benzimidazole to provide better solubility than **PCDTBT** at room temperature in organic solvents. It is possible to construct the quinoid form by using 2*H*-benzimidazole unit, to which dialkyl group can be introduced [12]. To obtain absorption in the longer wavelength region, bithiophene units without alkyl groups are incorporated in both of the monomers, which may result in low solubility of the polymers. The dihexyl

---

[*] Corresponding author. Tel.: +82 51 510 2203; fax: +82 51 516 7421.
E-mail address: hssuh@pusan.ac.kr (H. Suh).

0032-3861/$ – see front matter
doi:10.1016/j.polymer.2010.09.035

groups attached to the benzimidazole unit can improve the solubilities of the polymers. Polyfluorene (PF) [13], polycyclopentaphenanthrene (PCPP)[14] and polyphenylene (PPP)[11] have large band gaps and their alternating copolymers[15] with electron-deficient unit can provide large V_{oc} of the OPVs. The donor-acceptor type conjugated polymers were synthesized by Stille coupling reaction of 4,7-dibromo-2,2-dihexyl-2*H*-benzimidazole and donors including carbazole, 4*H*-cyclopenta[*def*]phenanthrene, fluorene and alkoxyphenylene. The photovoltaic properties of the polymers were investigated by fabrication of the polymer solar cells with the configuration of ITO/PEDOT:PSS/polymer:$PC_{71}BM/TiO_x$/Al.

2. Results and discussion

2.1. Synthesis and characterization

The general synthetic routes toward the monomers and polymers are outlined in Scheme 1. In the first step, 3,6-dibromobenzene-1,2-diamine (**1**)[16] was treated with 7-tridecanone (**2**)

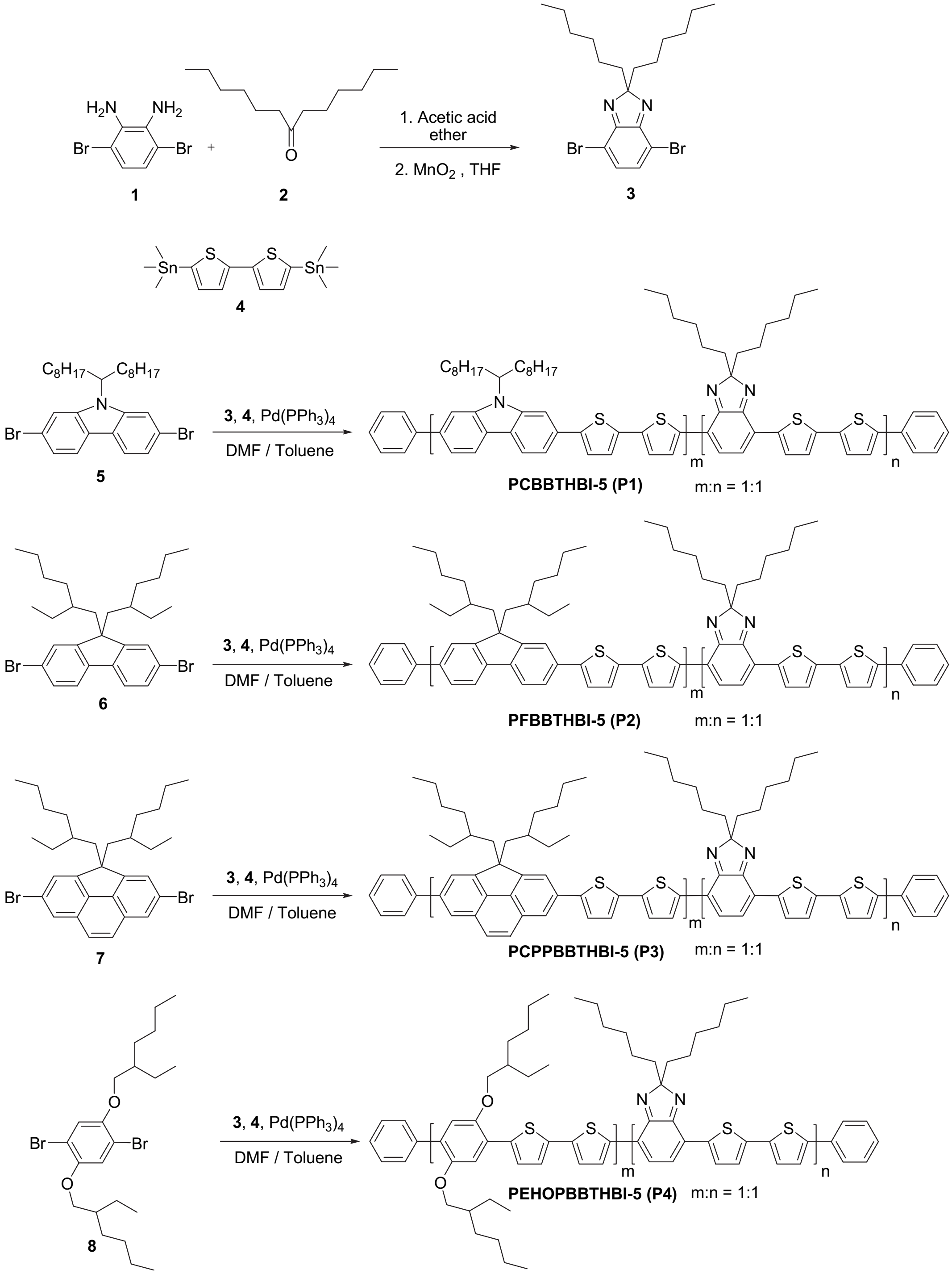

Scheme 1. Synthetic route for the synthesis of the monomers and polymers.

and acetic acid as catalyst to generate 2,2-dihexyl-2*H*-benzimidazole (**3**). Copolymers that consist of various monomers, 2,7-dibromo-9-(1-octylnonyl)-9*H*-carbazole (**5**) [7], 2,7-dibromo-9,9-bis(2-ethylhexyl)-9*H*-fluorene (**6**) [17], 2,6-dibromo-4,4-bis(2-ethylhexyl)-4*H*-cyclopenta[*def*]phenanthrene (7)[14,18] and 1,4-dibromo-2,5-bis[(2-ethylhexyl)oxy]-benzene (**8**) [19], as electron-rich units, 4,7-dibromo-2,2-dihexyl-2*H*-benzimidazole (**3**) as electron-deficient moiety, and 5,5′-bis(trimethylstannyl)-2,2′-bithiophene (**4**)[20] were synthesized by Pd(0)-catalyzed Stille coupling polymerization in toluene. The feed molar ratio of **3**, **4** and electron-rich units (**5**, **6**, **7** or **8**) is 1:2:1 to provide **P1**, **P2**, **P3** and **P4**, respectively. The actual molar ratios of the 2,2-dihexyl-2*H*-benzimidazole in the copolymers were calculated using elemental analysis and found to be very close to the feed molar ratio, as listed in Table 1. Caused by the lower reactivity of the HBI unit as compared to those of electron-rich units (**5**, **6**, **7**, and **8**) in the Suzuki reaction condition, the actual molar ratios of HBI unit incorporated in the polymers were slightly lower than the feeding ratios. All of the polymers show good solubility at room temperature in organic solvents such as chloroform, THF, chlorobenzene, and *o*-dichlorobenzene (ODCB). Even with two bithiophene units in the copolymers, the incorporation of dihexyl-substituent on 2*H*-benzimidazole enables them to have good solubility. Table 1 summarizes the polymerization results including molecular weight, polydispersity index (PDI) and thermal stability of the polymers. The number-average molecular weight (M_n) of 6100–10500 and weight-average molecular weight (M_w) of 12000–18800 with polydispersity index (PDI, M_w/M_n) of 1.7–2.0 of the resulting polymers were determined by GPC. The thermal properties of the polymers were characterized by both differential scanning calorimetry (DSC) and thermal gravimetric analysis (TGA). The Differential scanning calorimetry analysis was performed under a nitrogen atmosphere (50 mL/min) on a DSC 822 at heating rates of 10 °C/min. Thermal gravimetric analysis was performed with a Dupont 951 TGA instrument in a nitrogen atmosphere at a heating rate of 10 °C/min to 600 °C. The decomposition temperatures (T_d) are 384–423 °C for resulting polymers under N_2. The polymers showed good thermal stability with a glass transition temperature (T_g) of 70–105 °C, using DSC performed at a temperature range of 30–250 °C. The high thermal stability of the resulting polymers prevents the deformation of the polymer morphology and is important for organic photovoltaics (OPVs) application.

2.2. Optical and photoluminescence properties

The optical and photoluminescence properties of the polymer were investigated both in ODCB solution and in thin film. The absorption data for the polymers are shown in Fig. 1. Uniform polymer film was prepared on quartz plates by spin-casting from their ODCB solution at room temperature. The absorption spectra of polymers exhibited a maximum peak at about 439–466 nm in solution. The solid films show absorption bands with maximum peaks at about 442–479 nm and the absorption onsets at 529–575 nm, corresponding to band gaps of 2.16–2.34 eV. The film absorption spectra of the polymers were red-shifted around 3–13 nm as compared to those in solution. The solution and thin film of **P4** present absorption bands with maximum peak at 466 and 479 nm, respectively. The more red-shifted peak of **P4** as compared to those of other polymers is due to the stronger intramolecular charge transfer between the donors and dihexyl-2*H*-benzimidazole unit through the push-pull effect [21]. The dialkoxy-phenylene unit is more electron rich as compared to the other donors, caused by the electron-donating effect of the two oxygen atoms to improve the donor-acceptor-donor characteristics of the polymer backbone.

Table 1
Polymerization results and thermal properties of polymers.

Polymer	M_n[a]	M_w[a]	PDI[a]	DSC (T_g)	TGA (T_d)[b]	In the copolymer
P1	10000	18000	1.8	88	423	53.92:46.08
P2	10000	17000	1.7	105	407	54.78:45.22
P3	6100	12000	2.0	96	397	55.35:44.65
P4	10500	18800	1.8	70	384	53.17:46.17

[a] Molecular weight (M_w) and polydispersity (PDI) of the polymers were determined by gel permeation chromatography (GPC) in THF using polystyrene standards.
[b] Onset decomposition temperature (5% weight loss) measured by TGA under N_2.

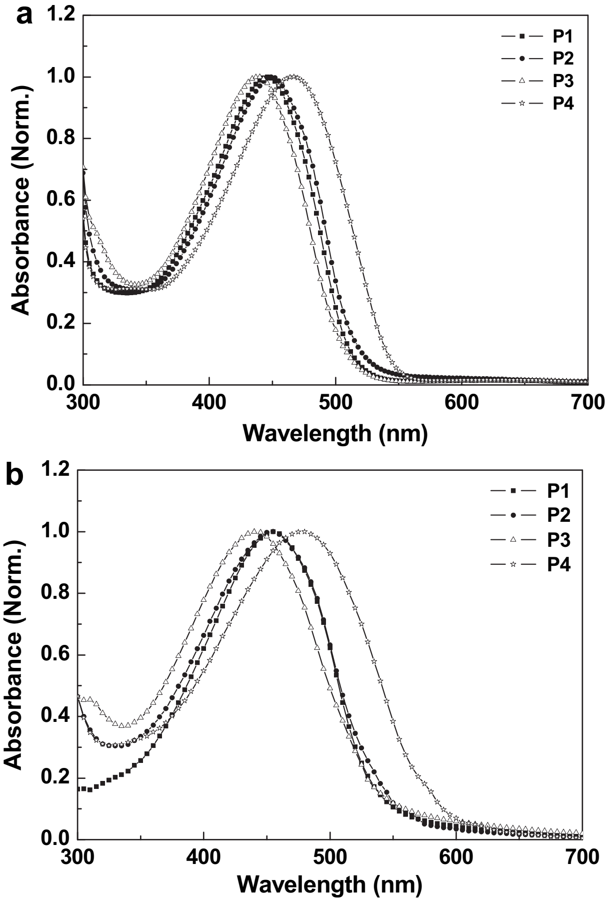

Fig. 1. UV–visible absorption spectra of polymers in ODCB solution (a), in the solid state (b).

2.3. Electrochemical properties

The electrochemical properties of the polymer were determined from the bandgap estimated from the absorption onset wavelength, and the HOMO energy level which was estimated from the cyclic voltammetry (CV). The CV was performed with a solution of tetrabutylammonium tetrafluoroborate (Bu_4NBF_4) (0.10M) in acetonitrile at a scan rate of 100 mV/s at room temperature under argon atmosphere. A platinum electrode (~0.05 cm^2) coated with a thin polymer film was used as the working electrode. Pt wire and $Ag/AgNO_3$ electrode were used as the counter electrode and reference electrode, respectively. The energy level of the $Ag/AgNO_3$ reference electrode (calibrated by the Fc/Fc^+ redox system) was

4.8 eV below the vacuum level. The CV spectra are shown in Fig. 2, and the oxidation potentials derived from the onsets of electrochemical p-doping are summarized. HOMO and LUMO levels were calculated according to the empirical formula ($E_{\mathrm{HOMO}} = -([\mathrm{E_{onset}}]^{\mathrm{ox}} + 4.8)$ (eV) and ($E_{\mathrm{LUMO}} = -([\mathrm{E_{onset}}]^{\mathrm{red}} + 4.8)$ (eV), respectively. The polymers, **P1**, **P2, P3** and **P4**, exhibited the absorption onset wavelengths of 534, 540, 529 and 575 nm in solid thin film, which corresponds to band gaps of 2.32, 2.30, 2.34 and 2.16 eV, respectively. The polymers exhibit irreversible processes in an oxidation scan. The oxidation onsets of the polymers, **P1**, **P2, P3** and **P4**, were estimated to be 0.71, 0.65, 0.71, and 0.48 V, which correspond to HOMO energy levels of −5.51, −5.45, −5.51 and −5.28 eV, respectively. The HOMO level of **P4** was increased owing to alkoxyphenylene unit with oxygen atoms with electron-donating effect. The reduction potential onsets of polymers, **P1**, **P2, P3** and **P4**, are −1.56, −1.31, −1.52 and −1.22 V, which corresponds to LOMO energy levels of −3.24, −3.49, −3.28 and −3.58 eV, respectively. The electrochemical band gaps, calculated from cyclic voltammetry data, are about 1.70–2.27 eV, somewhat lower than the optical band gaps estimated from the onset wavelengths of the absorption spectra. Fig. 3 illustrates a diagram of energy levels of the polymers as compared to that of $PC_{71}BM$ and the work functions of indium tin oxide (ITO), poly(3,4-ethylenedioxythiophene): poly(styrenesulfonate) (PEDOT:PSS), and aluminum (Al) used in OPV devices.

2.4. *Polymer photovoltaic properties*

The OPVs were fabricated by spin-casting of ODCB solution of $PC_{71}BM$/polymers. All polymers were applied as donors into a conventional BHJ type OPV device with $PC_{71}BM$ as acceptor, which has been widely used for this purpose. Typical J-V characteristics of devices with the configuration of ITO/PEDOT:PSS (40 nm)/polymer:$PC_{71}BM$(1:4) (80 nm)/TiOX (10 nm)/Al (100 nm) under AM 1.5 G irradiation (100 mW/cm^2) are depicted in Fig. 4. The photovoltaic parameters for all the polymers, including open-circuit voltage (VOC), short-circuit current density (JSC), fill factor (FF), and power conversion efficiency (PCE) are summarized in Table 2. The devices comprising **P1**, **P2**, and **P3** with $PC_{71}BM$ showed an open-circuit voltage (VOC) of 0.39, 0.44 and 0.34 V, a short-circuit current density (JSC) of 1.31, 2.45 and 1.42 mA/cm^2, and a fill factor (FF) of 0.40, 0.37 and 0.36, giving a power conversion efficiency of 0.21, 0.39 and 0.17%, respectively. The device with **P4**:$PC_{71}BM$ blend demonstrated a VOC value of 0.59 V, a JSC value of 6.43 mA/cm^2, and an FF of 0.39, leading to the efficiency of 1.46%, improved performance relative to the other polymers. The incident photon-to-current efficiency (IPCE) spectra of the photovoltaic devices from polymer:$PC_{71}BM$ blends are presented in Fig. 5. The IPCE spectra of the polymers show maxima of 10.37% at 460 nm for **P1**, 18.68% at 460 nm for **P2**, 6.63% at 470 nm for **P3** and 53.41% at 430 nm for **P4**. The enhanced efficiency of **P4** results from the higher IPCE value between 400 and 700 nm as compared to the cases of other polymers.

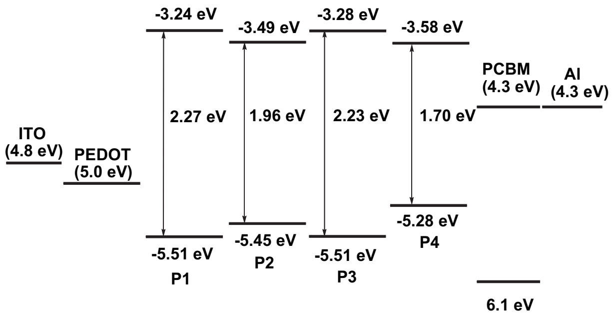

Fig. 3. Enegy-level diagram showing the HOMO and LUMO energy levels of polymers and $PC_{71}BM$.

The AFM topographies of polymer blends (polymer: $PC_{71}BM = 1:4$ w/w) were investigated by the casting films of ODCB solutions as shown in Fig. 6 where the images were obtained in a surface area of 5 × 5 μm^2 by the tapping mode. The root mean squares (rms) roughness of the blend film of **P1**, **P2, P3** and **P4** are 0.41, 0.29, 0.32 and 0.52 respectively, and no significant aggregation is formed.

3. Conclusions

New polymers, **P1**, **P2, P3** and **P4** utilizing a new accepter, dihexyl-2*H*-benzimidazole, were synthesized to show good solubilities at room temperature in organic solvents, even with two di-thiopene units in the structures. The advantage of dihexyl-2*H*-benzimidazole compared to the benzothiadiazole moiety of **PCDTBT** is to improve the solubility of the polymer while keeping the coplanarity of the backbone. The spectra of the solid films show absorption bands with maximum peaks at about 442–479 nm and the absorption onsets at 529–575 nm, corresponding to band gaps of 2.16–2.34 eV. The device with **P4**:$PC_{71}BM$ blend demonstrated a V_{OC} value of 0.59 V, a J_{SC} value of 6.43 mA/cm^2, and a *FF* of 0.39,

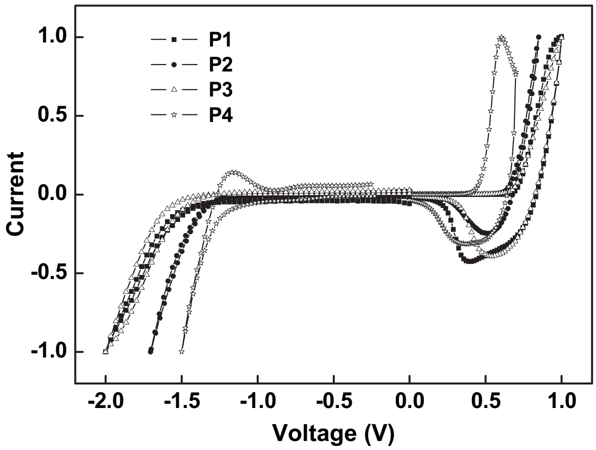

Fig. 2. Electrochemical properties of polymers.

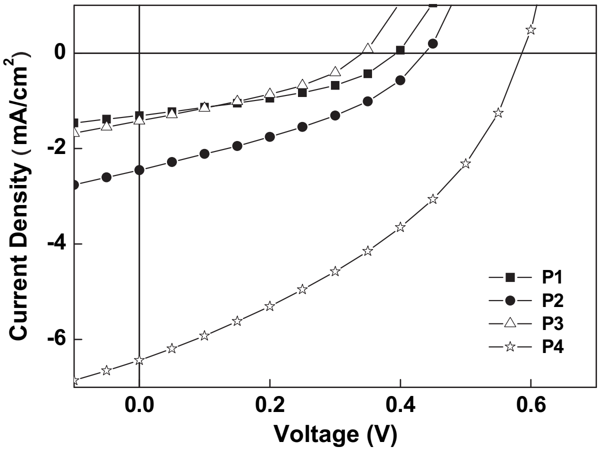

Fig. 4. Current density-potential characteristics of the polymers solar cells under the illumination of AM 1.5, 100 mW/cm^2.

Table 2
Photovoltaic properties and TFT characteristics of the polymer solar cells.

Polymers	V_{OC} (V)	J_{SC} (mA/cm^2)	*FF*	PCE (%)
P1	0.39	1.31	0.40	0.21
P2	0.44	2.45	0.37	0.39
P3	0.34	1.42	0.36	0.17
P4	0.59	6.43	0.39	1.46

leading to the efficiency of 1.46%. The higher efficiency of **P4** as compared to those of other polymers is due to the stronger intramolecular charge transfer, which is contributed to the phenylene unit with electron-rich di-alkoxy groups. This indicates that the narrow bandgap copolymer **P4** is a viable electron donor material for polymeric solar cells.

4. Experimental Section

General. All reagents were purchased from Aldrich or TCI, and used without further purification. Solvents were purified by normal procedure and handled under moisture-free atmosphere. ^{1}H and ^{13}C NMR spectra were recorded with a Varian Gemini-300 (300 MHz) spectrometer and chemical shifts were recorded in ppm units with TMS as the internal standard. Flash column chromatography was performed with Merck silica gel 60 (particle size 230–400 mesh ASTM) with ethyl acetate/hexane or methanol/methylene chloride gradients unless otherwise indicated. Analytical thin layer chromatography (TLC) was conducted using Merck 0.25 mm silica gel 60F pre-coated aluminum plates with fluorescent indicator UV254. High resolution mass spectra (HRMS) were recorded on a JEOL JMS-700 mass spectrometer under electron impact (EI) or fast atom bombardment (FAB) conditions in the Korea Basic Science Institute (Daegu). Molecular weights and polydispersities of the polymers were determined by gel permeation chromatography (GPC) analyses with polystyrene standard calibration. The UV–vis absorption spectra were recorded by a Varian 5E UV/VIS/NIR spectrophotometer, while the Oriel InstaSpec IV CCD detection system with xenon lamp was used for the photoluminescence and electroluminescence spectra measurements. Solar cells were fabricated on an indium tin oxide (ITO)-coated glass substrate with the following structure; ITO-coated glass substrate/poly(3,4-ethylenedioxythiophene)(PEDOT:PSS)/polymer: PC$_{71}$BM/TiO$_x$/Al. The ITO-coated glass substrate was first cleaned with detergent, ultrasonicated in acetone and isopropyl alcohol, and subsequently dried overnight in an oven. PEDOT:PSS (Baytron PH) was spin-cast from aqueous solution to form a film of 40 nm thickness. The substrate was dried for 10 min at 140 °C in air and then transferred into a glove box to spin-cast the charge separation layer. A solution containing a mixture of polymer:PC$_{71}$BM (1:4) in dichlorobenzene solvent with concentration of 7wt/ml % was then spin-cast on top of the PEDOT/PSS layer. The film was dried for 60 min at 70 °C in the glove box. The TiO$_x$ precursor solution diluted by 1:200 in methanol was spin-cast in air on top of the polymer:PC$_{71}$BM layer (5000rpm for 40 s). The sample was heated at 80 °C for 10 min in air. Then, an aluminum (Al, 100 nm) electrode was deposited by thermal evaporation in a vacuum of about 5×10^{-7} Torr. Current density-voltage (J-V) characteristics of the devices were measured using a Keithley 236 Source Measure Unit. Solar cell performance utilized an Air Mass 1.5 Global (AM 1.5 G) solar simulator with an irradiation intensity of 1000 W m^{-2}. An aperture (12.7 mm^2) was used on top of the cell to eliminate extrinsic effects such as cross-talk, waveguiding, and shadow effects, etc. The spectral mismatch factor was calculated by comparison of solar simulator spectrum with AM 1.5 spectrum at room temperature. The IPCE is a measure of the photon to electron conversion efficiency at a particular irradiation wavelength (equation (1)).

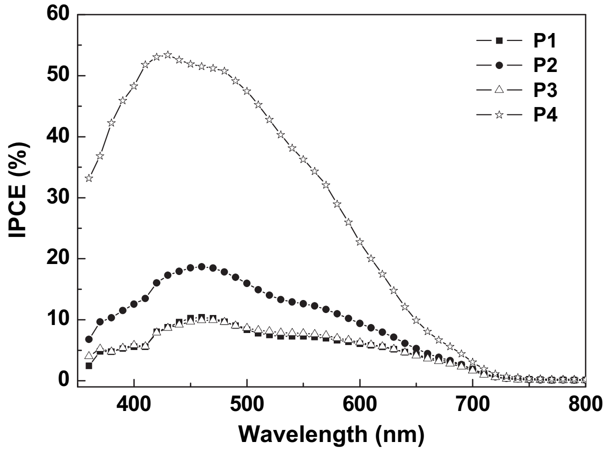

Fig. 5. IPCE curves of the polymer solar cells under the illumination of AM 1.5, 100 mW/cm^2.

$$\mathrm{IPCE} = (1240 \times J_{SC}) / (\lambda_i \times \mathrm{Pin}) \qquad (1)$$

*Synthesis of 4,7-dibromo-2,2-dihexyl-2H-benzimidazole (**3**)*. To a stirred solution of 3,6-dibromobenzene-1,2-diamine (**1**) (10 g, 37.65 mmol), 7-tridecanone (**2**) (10 mL), and acetic acid (10 mL) were dissolved in diethyl ether (200 mL) and heated to 50 °C overnight. After the reaction mixture was cooled to room temperature, water and ethyl acetate were added. The aqueous phase was extracted with ethyl acetate and combined organic layer were dried over MgSO$_4$. The solvent was removed under vacuum and the residue was purified by column chromatography to give 4,7-dibromo-2,2-dihexyl-2,3-dihydro-1*H*-benzimidazole. To a stirred solution of 4,7-dibromo-2,2-dihexyl-2,3-dihydro-1*H*-benzimidazole in 50 mL of tetrahydrofuran (THF) at room temperature was added MnO$_2$ (10 g). After 3 h, the solid was filtered and washed with THF. The combined organic phase was concentrated under reduced pressure and purified by flash column chromatography to give 4.8 g of compound **2** as yellow powder. mp 60 °C; ^{1}H NMR (300 MHz, CDCl$_3$): δ (ppm) 0.83 (t, 6H, $J = 6.87$ Hz), 0.92–0.88 (m, 4H), 1.25–1.17 (m, 12H), 2.24–2.18 (m, 4H), 7.20 (s, 2H); ^{13}C NMR (75 MHz, CDCl$_3$): δ (ppm) 14.26, 22.78, 23.72, 29.62, 31.74, 35.77, 109.92, 118.42, 136.12, 157.87. HRMS(*m/z*, FAB$^+$) calcd for C$_{19}$H$_{29}$Br$_2$N$_2$ 443.0697, found 443.0695.

General procedure of copolymerization. Carefully purified 4,7-dibromo-2,2-dihexyl-2*H*-benzimidazole (**3**), 5,5′-bis(trimethylstannyl)-2,2′-bithiophene (**4**), (PPh$_3$)$_4$Pd(0) (3 mol%), and various donors, 2,7-dibromo-9-(1-octylnonyl)-9*H*-carbazole (**5**), 2,7-dibromo-9,9-bis(2-ethylhexyl)-9*H*-fluorene (**6**), 2,6-dibromo-4,4-bis(2-ethylhexyl)-4*H*-cyclopenta[*def*]phenanthrene (**7**) and 1,4-dibromo-2,5-bis[(2-ethylhexyl)oxy]-benzene (**8**) were dissolved in a mixture of toluene and DMF. After refluxing for 72 h, trimethyl(phenyl)tin was added to the reaction mixture. After refluxing for additional 12 h, the reaction mixture was treated with bromobenzene and refluxed overnight to complete the end-capping. After cooling to room temperature, the mixture was poured into methanol. After filtration, the resulting solid material was reprecipitated using 1.0 L of methanol several times to remove catalyst residues. The resulting polymers were soluble in THF, CHCl$_3$, *o*-dichlorobenzene (ODCB) and toluene. The ratios of 5,5′-bis(trimethylstannyl)-2,2′-bithiophene (**4**), 4,7-dibromo-2,2-dihexyl-2*H*-benzimidazole (**3**), and various donors (**5**, **6**, **7** or **8**) were always kept as 2:1:1.

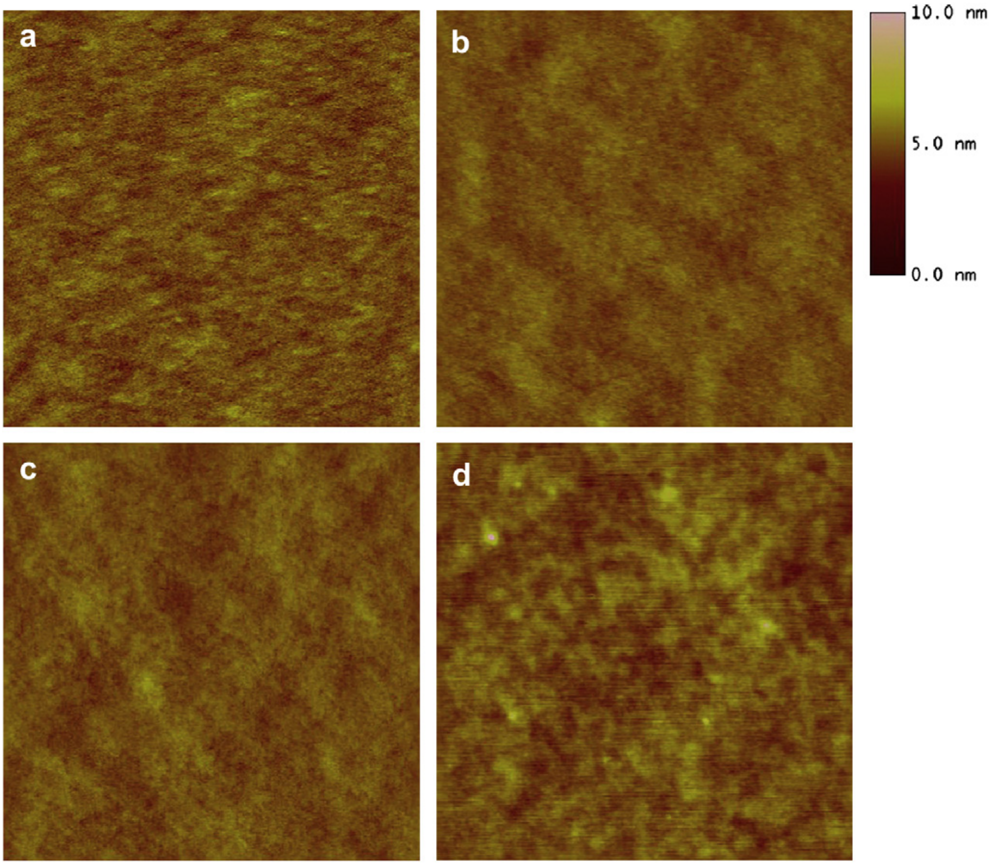

Fig. 6. Atomic force microscopy images of **P1**/PC$_{71}$BM (a), **P2**/PC$_{71}$BM (b), **P3**/PC$_{71}$BM (c), and **P4**/PC$_{71}$BM (d).

*PCBBTHBI-5 (**P1**)*

^{1}H NMR (300 MHz, CDCl$_3$): δ (ppm) 0.83, 1.15, 1.25, 2.00, 2.35, 2.91, 4.00, 4.62, 6.91, 7.35, 7.50, 7.61, 7.78, 8.06. Anal. Calcd for $C_{32}H_{38.5}N_{1.5}S_2$: C, 75.61; H, 7.64; N, 4.14. Found: C, 73.48; H, 7.51; N, 3.81.

*PFBBTHBI-5 (**P2**)*

^{1}H NMR (300 MHz, CDCl$_3$): δ (ppm) 0.76, 0.85, 0.88, 1.08, 1.25, 1.35, 1.99, 2.89, 3.99, 7.05, 7.32–7.68, 8.07. Anal. Calcd for $C_{32}H_{38}N_1S_2$: C, 76.75; H, 7.65; N, 2.80. Found: C, 71.35; H, 6.85; N, 2.53.

*PCPPDDTHBI-5 (**P3**)*

^{1}H NMR (300 MHz, CDCl$_3$): δ (ppm) 0.56, 0.64, 0.81, 1.15, 1.26, 1.30, 1.41, 1.53, 1.68, 2.26, 2.90, 4.01, 7.03, 7.30, 7.41, 7.54, 7.62, 7.64, 7.83, 8.05, 9.48. Anal. Calcd for $C_{33}H_{38}N_1S_2$: C, 77.29; H, 7.47; N, 2.73. Found: C, 73.59; H, 7.20; N, 2.44.

*PEHOPBBTHBI-5 (**P4**)*

^{1}H NMR (300 MHz, CDCl$_3$): δ (ppm) 0.92, 1.01, 1.59, 1.90, 2.90, 3.03, 4.04, 7.02, 7.16, 7.28, 7.41–7.60, 8.10. Anal. Calcd for $C_{28.5}H_{37}N_1O_1S_2$: C, 72.25; H, 7.87; N, 2.96; O, 3.38. Found: C, 68.95; H, 7.31; N, 2.77; O, 3.54.

Acknowledgements

This work was supported by the National Research Foundation of Korea (NRF) grant funded by the Korea government (MEST) (2010-0015069).

References

[1] Aernouts T, Aleksandrov T, Girotto C, Genoe J, Poortmans J. Appl Phys Lett 2008;92:033306/1–033306/3.
[2] (a) Krebs FC, Gevorgyan SA, Alstrup J. J Mater Chem 2009;19:5442–51;
(b) Sacriciftci NS, Smilowitz L, Heeger AJ, Wudl F. Science 1992;258:1474–6.
[3] Huang F, Chen KS, Yip HL, Hau SK, Acton O, Zhang Y, et al. J Am Chem Soc 2009;131:13886–7.
[4] Hou J, Chen HY, Zhang S, Li G, Yang Y. J Am Chem Soc 2008;130:16144–5.
[5]. (a) Liang Y, Wu Y, Feng D, Tsai ST, Son HJ, Li G, et al. J Am Chem Soc 2009;131:56–7;
(b) Brabec CJ, Sariciftci NS, Hummelen JC. Adv Funct Mater 2001;11:15–26.
[6] Park SH, Roy A, Beaupre S, Cho S, Coates N, Moon JS, et al. Nat Photonics 2009;3:297–303.
[7] Blouin N, Michaud A, Leclerc M. Adv Mater 2006;19:2295–300.
[8] (a) Wang E, Wang M, Wang L, Duan C, Zhang J, Cai W, et al. Macromolecules 2009;42:4410–5;
(b) Huang F, Chen K, Yip H, Hau SK, Acton O, Zhang Y, et al. J Am Chem Soc 2009;131:13886–7.
[9] Tantiwiwat M, Tamayo A, Luu N, Dang XD, Nguyen TQ. J Phys Chem C 2008;112:17402–7.
[10] Karikomi M, Kitamura C, Ranaka S, Yamashita Y. J Am Chem Soc 1995;117:6791–2.
[11] Liu CL, Tsai JH, Lee WY, Chen WC, Jenekhe SA. Macromolecules 2008;41:6952–9.
[12] Song S, Jin Y, Feng D, Park SH, Cho S, Kim I, Lee K, Heeger AJ, Suh H. J Mater Chem 2010;20:6517–23.
[13] Jin Y, Kim JY, Park SH, Kim J, Lee S, Lee K, et al. Polymer 2005;46:12158–65.
[14] (a) Suh H, Jin Y, Park SH, Kim D, Kim J, Kim C, et al. Macromolecules 2005;38:6285–9;

(b) Park SH, Jin Y, Kim JY, Kim SH, Kim J, Suh H, et al. Adv Funct Mater 2007;17:3063–8.
[15] Kim J, Park SH, Cho S, Jin Y, Kim J, Kim I, et al. Polymer 2010;51:390–6.
[16] Tsami A, Yang XH, Galbrecht F, Farrell T, Li H, Adamczyk S, et al. J Polym Sci Part A Polym Chem 2007;45:4773–85.
[17] Grigalevicius S, Ma L, Xie Z, Scherf U. J Polym Sci Part A Polym Chem 2006;44:5987–94.
[18] Song S, Jin Y, Kim J, Park SH, Kim SH, Lee K, et al. Polymer 2008;49: 5643–9.
[19] Irvin JA, Schwendeman I, Lee Y, Abboud KA, Reynolds JR. J Polym Sci Part A Polym Chem 2001;39:2164–78.
[20] Fong HH, Pozdin VA, Amassian A, Malliaras GG, Smilgies D, He M, et al. J Am Chem Soc 2008;130:13202–3.
[21] Shi CJ, Yao Y, Yang Y, Pei QB. J Am Chem Soc 2006;128:8980–6.